Electrochemical and Solid-State Letters, **8** (4) G85-G88 (2005)
1099-0062/2005/8(4)/G85/4/$7.00 © The Electrochemical Society, Inc.

High Optical Quality Nanoporous GaN Prepared by Photoelectrochemical Etching

A. P. Vajpeyi,[a] S. J. Chua,[a,b] S. Tripathy,[b,*,z] E. A. Fitzgerald,[a,c] W. Liu,[b] P. Chen,[b] and L. S. Wang[b]

[a]*Singapore-MIT Alliance, National University of Singapore, Singapore 117576*
[b]*Institute of Materials Research and Engineering, Singapore 117602*
[c]*Department of Materials Science and Engineering, Massachusetts Institute of Technology, Cambridge, Massachusetts 02139, USA*

Nanoporous GaN films are prepared by ultraviolet assisted electrochemical etching using HF solution as an electrolyte. To assess the optical quality and morphology of these nanoporous films, microphotoluminescence, micro-Raman scattering, scanning electron microscopy (SEM), and atomic force microscopy (AFM) techniques have been employed. SEM and AFM measurements revealed an average pore size of about 85-90 nm with a transverse dimension of 75-85 nm. As compared to the starting as-grown GaN film, porous layer exhibits a substantial photoluminescence intensity enhancement with a partial relaxation of compressive stress. Such a stress relaxation is further confirmed by the red shifted E_2^{high} phonon peak in the Raman spectrum of porous GaN.
 [DOI: 10.1149/1.1861037]

Manuscript submitted October 26, 2004; revised manuscript received December 2, 2004.
Available electronically February 10, 2005.

Porous semiconductors have been widely studied in the last decade due to their unique optical properties compared to the bulk materials. Porous semiconductors successfully prepared from Si,[1,2] GaAs,[3-6] GaP,[7-9] and InP[10-12] exhibit tunable properties that can be explored to fabricate new sensing devices. The main objective of this research was to control the emission properties of the porous semiconductors by controlling the pore dimension. Porous layer can also be used as a buffer or intermediate layer for strain management during epitaxial regrowth. Such a growth method may reduce or redistribute the defect density in the epitaxial layer, leading to a high-quality stress-free layer on porous template. GaN and its related nitrides are generally grown on sapphire (13.6% lattice mismatch) or SiC substrates (4% lattice mismatch), where larger lattice mismatch introduces a high density of dislocations. However, reducing the dimensions of these structures to nanoscale can extend the range of properties of nitride materials. For example, nanostructured GaN can have a reduced defect density and enhanced strain relaxation as compared to epitaxial GaN films, and the optical properties of such materials can be tailored to suit various device requirements.

It has been reported that GaN grown on nanoporous SiC and nanoporous GaN shows improved chemical and optical quality.[13-15] Although porous GaN offers a good alternative for growing a high-quality stress-free over layer, little work has been done to date. Recently, few studies on the bandgap and morphology control in porous GaN through electroless wet chemical and photoelectrochemical etching are reported.[16-20] A method to prepare ordered nanopores in GaN films by inductively coupled plasma (ICP) etching using anodic alumina templates as etching mask is also demonstrated recently.[21] Photoelectrochemical etching would be more suitable as a cost effective method to produce high-density nanopores with pore size <100 nm. The pore size, etching depth, or the transverse dimension of the pores can be easily controlled by varying the etching/anodization conditions. If a much higher PL signal can be extracted from porous GaN compared to the as-grown material, such porous template would be suitable as a pumping source or suitable host for multiple light emitting layers that emit emission energy lower than the bandgap of GaN. Apart from improved optical pumping, such a template will reduce the dislocation density of the layers to be grown on top of it via nano-ELO process.[14,15] In this paper, we report fabrication and properties of nanoporous GaN prepared by ultraviolet (UV)-assisted electrochemical etching using HF solution as an electrolyte. A significant photoluminescence (PL) intensity enhancement is observed from porous GaN films. The red-shifted PL emission observed from porous GaN when compared with the as grown epilayer indicates a relaxation of compressive stress. This is further confirmed by micro-Raman spectroscopy.

The GaN layers were grown by low-pressure metallorganic chemical vapor deposition (MOCVD) on sapphire (0001) substrates. A 25 nm thick buffer layer of GaN was first grown at 500°C and, subsequently, a 0.5 μm thick undoped GaN layer followed by a 2.0 μm thick Si-doped n-GaN layer were grown at 1050°C. The carrier concentration in the upper layer was 1.2×10^{18} cm^{-3} as determined by Hall measurement. For a comparative study, we have also taken an unintentionally doped 2.5 μm thick GaN with a carrier concentration of 1.2×10^{16} cm^{-3}. These GaN layers were subjected to UV assisted electrochemical etching using 49%(HF:H_2O = 2:1) buffered HF solution as an electrolyte. Al films were evaporated at one corner of the GaN surface for contact and Pt electrode was used during various anodization conditions. Etching was performed using front side illumination with 350 W UV lamp. The anodization current was varied from 20-50 mA/cm^2 for different samples with a constant etch time of 60 min. Samples were chemically cleaned to remove surface contaminants and oxides well before any characterization. UV assisted electrochemical etching depends on the photo generated electronhole pairs, where etching proceeds through the oxidation and subsequently dissolution of the semiconductor surface. Holes play an important role in converting the surface atom into the higher oxidation state. The absorption of incident radiation greatly increase the supply of holes available at the surface to participate in the oxidation reaction, resulting in significantly enhanced etch rate. During the etch process, bubble formation is observed due to the nitrogen evolution. The dissolution reaction is given by, $2GaN + 6h^+ \rightarrow 2Ga^{+3} + N_2\uparrow$. Figure 1 shows the top view scanning electron microscopy (SEM) image of the porous GaN surface prepared using varying etching conditions. The average pore and the GaN crystallite size are <100 nm. Optimized etching conditions in n-GaN layer gave an average pore size of about 85-90 nm with a transverse dimension of 75-85 nm, which is confirmed by cross-sectional SEM measurements. In the unintentionally doped GaN sample, the pore depth was found to be only 40 nm even if using a higher anodization current density. The pore depth is much higher in Si-doped sample compared with undoped samples due to the higher conduction in Si-doped GaN. Higher conductivity helps in the formation of deeper pores due to higher etch rate. Pore size is difficult to control during such etching processes but changes can be observed by varying etching parameter, *e.g.*, current density, etch time, carrier concentration, or solution concentration. The average pore size varies significantly (70-100 nm) based on the quality of the starting GaN epilayers and an increased anodization current density

* Electrochemical Society Active Member.
z E-mail: tripathy-sudhiranjan@imre.a-star.edu.sg

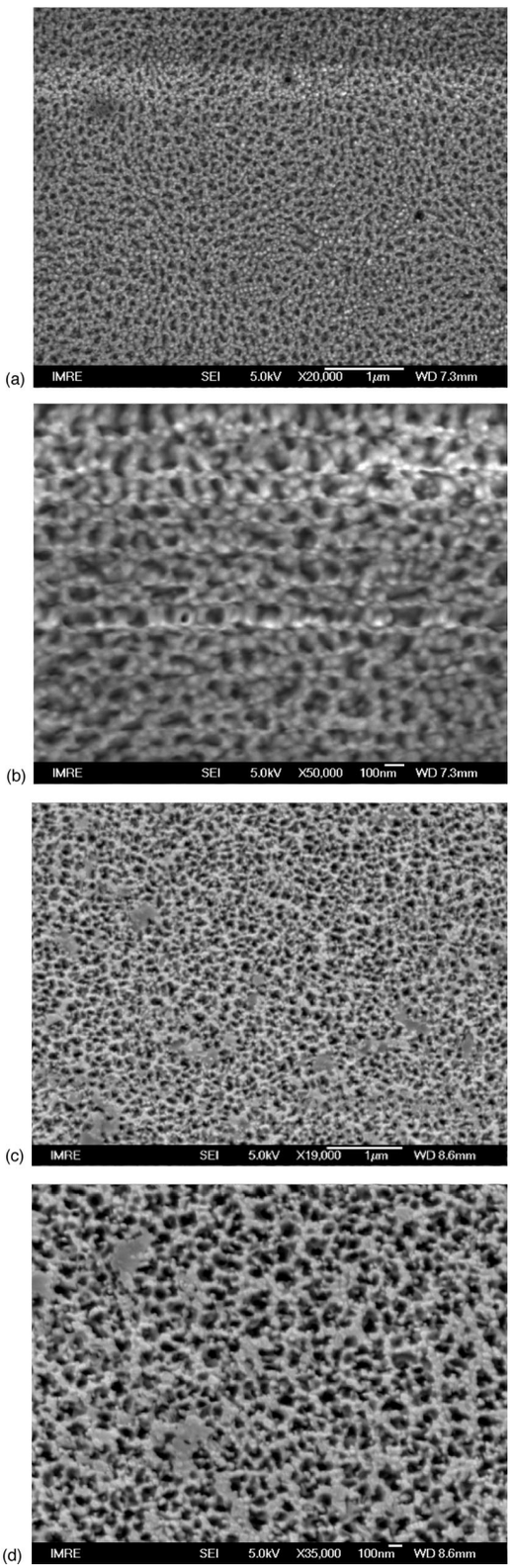

Figure 1. SEMs of porous GaN prepared under variable etching conditions. (a) Low magnification image of porous GaN prepared from n-GaN with 49% HF solution ($HF:H_2O = 2:1$) and anodization current density 20 mA/cm^2. (b) High magnification image of the porous n-GaN sample. (c) Low magnification image of porous layer prepared from unintentionally doped GaN with 49% HF solution ($HF:H_2O = 2:1$), anodization current density 50 mA/cm^2. (d) High magnification image of the porous undoped GaN sample.

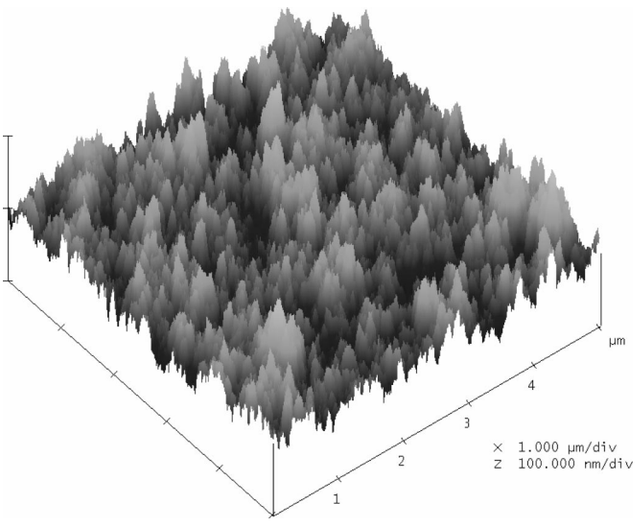

Figure 2. 5.0 × 5.0 μm 3D-AFM of nanoporous GaN.

led to widening of the pores. We have also carried out a comparative study of surface morphology of porous GaN prepared by both photoelectrochemical and UV-assisted electroless etching. The pore size is somewhat more uniform in photoelectrochemical etching.

Figure 2 shows the 3D-atomic force microscopy (AFM) topography of the porous GaN using a Digital Nanoscope III set up. From the section line scan, we estimate an average pore depth of ~75 nm in Si-doped sample. However, the AFM tip cannot probe the exact pore depth accurately due to the tip size limitation. Cross-sectional SEM measurements were performed to measure the pore depth more accurately. From cross-sectional SEM, an average pore depth of ~80 nm is observed for the Si-doped GaN sample. The density of the nanopores is much higher as evident from the SEM image. Such large area nanoporous GaN prepared by this method may be suitable for regrowth of GaN and high Al content AlGaN based device layers. The optical quality of the porous GaN samples prepared by this method was investigated by high-spatial resolution PL and Raman microscopy. PL spectra were recorded using a Renishaw 2000 micro-PL setup and using 325 nm line excitation from a He-Cd laser. Normalized PL intensity signal is recorded using a 40 times magnification UV-objective lens, where the laser beam is focused to 2 μm spot size. Micro-Raman measurements were carried out using a JYT64000 triple spectrograph attached to a liquid nitrogen cooled CCD camera for spectral imaging. The 514.5 nm line of an Ar^+ laser was used as a source for Raman excitation. The spatial and spectral resolution of the Raman set up is 1.0 and 0.2 cm^{-1}, respectively.

Figure 3 shows the room-temperature micro-PL spectra recorded from the Si-doped nanoporous GaN and the as-grown GaN epilayer. The room temperature near-band-edge PL peaks are centered around 3.42 eV. The PL spectrum recorded from porous film shows a uniform PL lineshape with a slight broadening toward the low-energy side. The slight broadening relative to the GaN epilayer emission could be due to incorporation of impurity-induced disorder or surface defects during etching. At room temperature, a significant enhancement of PL intensity was observed from the porous GaN when compared to the as-grown GaN epilayer. To investigate the improved emission properties of nanoporous GaN further, we have also carried out low-temperature PL measurements. Figure 3 also shows PL spectra recorded at 77 and 5 K from the porous GaN and the as-grown epilayer where a dominated free-excitonic transition FX(A) is observed from both the samples. A two-fold intensity enhancement is clearly observed for the free exciton (FX(A):3.476 eV at 5 K) lines from nanoporous film, while the free exciton peak for as-grown is at 3.481 eV. A red shift of about 4.8 ± 0.5 meV is observed for the FX(A) transition from the nanoporous GaN when

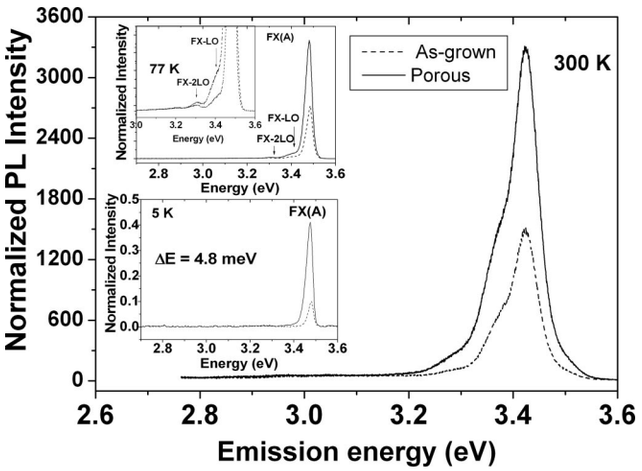

Figure 3. Micro-PL spectra of porous GaN and as grown GaN. Inset shows spectra recorded at 77 and 5 K.

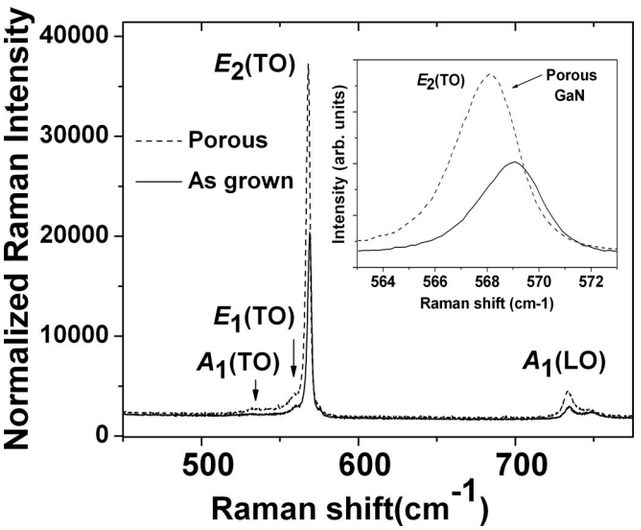

Figure 4. Micro-raman spectra recorded from as grown and porous GaN epilayer. Inset: the observed red shift for E_2^{high} phonon from porous film.

compared to the as-grown GaN epilayer. Such a red-shifted emission can be associated with partial relaxation of compressive stress in the nanoporous film. The improved PL intensity observed from porous GaN can be attributed to the reduction of surface pit density and extraction of more photons by light scattering off the sidewalls of the GaN crystallites. Although the outcoupling efficiency is much better on a roughened surface, we believe that etching through the dislocation cores and surface related traps could also lead to an enhancement of band-edge PL. This is further confirmed from the X-ray diffraction (XRD) measurements. In addition, we have also observed phonon replicas of FX(A) line such as FX-LO and FX-2LO peaks from 77 K micro-PL spectrum. The donor-acceptor pair emissions are also absent in the PL spectra. Yellow luminescence (YL), which is commonly observed in the PL spectrum of defective GaN around 2.2-2.3 eV, was also very weak in both porous and as grown film. Etching can lead to a nonstoichiometric GaN surface with C_N and O_N related vacancy-impurity complexes at the underlying etched surfaces. Because underlying GaN etched surface can contribute to the PL, the actual PL intensity may be quenched somewhat due to etching and creation of surface defects. The higher luminescience property of the nanoporous film indicates that such a template may have good potential for GaN based luminescent or sensing device.

We have also studied the evolution of integrated FX(A) PL intensity in porous GaN with temperature. The experimental data point were fitted according to Arrhenius equation

$$I(T) = \frac{I(0)}{1 + C\ \exp(-E_A/kT)} \quad [1]$$

where $I(T)$ is the intensity at temperature T, $I(0)$ is the intensity at 0 K, and E_A is the activation energy. From nanoporous GaN, an activation energy of 26 meV is estimated from the best-fitted curve for temperature range 5-300 K. For the as grown film, the activation energy is same as the porous film. Such observation agrees well with the reported value of activation energy of GaN nanocoloumns prepared by photoelectrochemical etching.[14] The temperature dependence of the emission energy for porous and the as grown GaN are well fitted by Varshni's equation[22]

$$E_g(T) = E_g(0) - \alpha\frac{T^2}{\beta + T} \quad [2]$$

where $E_g(0)$ is the FX(A) energy at 0 K, and α and β are the Varshni's thermal coefficients. For nanoporous GaN, the best fitted values obtained from least square fitting are given by $E(0) = 3.484$ eV, $\alpha = 7.0 \times 10^{-4}$ and $\beta = 700$ K, whereas for as-grown GaN, the parameters are given by $E(0) = 3.490$ eV, $\alpha = 7.6 \times 10^{-4}$ and $\beta = 680$ K. Because Varshni coefficient β is associated with the Debye temperature, there is no significant change in the Debye temperature expected from porous GaN. The energy shift between porous and as-grown GaN sample can be used to quantify the amount of stress relaxation. Using the value of the proportionality factor $K = 21.2 \pm 3.2$ meV/GPa[23] for the stress-induced PL peak shift, a compressive stress relaxation of about 0.22 ± 0.02 GPa is estimated. This observation also agrees well with micro-Raman analyses of the porous GaN.

To further investigate the quality of the porous GaN, XRD rocking curves were measured. The angular distribution of the (0002) reflection planes was measured with Cu$K\alpha$ radiation under symmetric Bragg reflection condition. The full width at half-maximum (fwhm) of the XRD rocking curve can provide information about crystalline quality. The fwhm of ω-2θ scan rocking curves of porous GaN shows only an increase of about 8 arc sec, which indicates that the porous layer is of comparable quality as the as grown epilayer even after anodization. The angular distribution of the (101) reflection plane was also measured. The fwhm of ω-2θ scan for (101) refection plane is related to all type of dislocations including edge, screw and mix dislocations. The fwhm of this rocking curve for Si-doped porous GaN is about 45 arc sec lower than the as-grown GaN, which is direct evidence of reduction in dislocation density in porous GaN. In addition, using XRD, we have also estimated the lattice constants of the porous ($c_{porous} = 5.195$ Å, $a_{porous} = 3.180$ Å) and as-grown epilayer ($c_{as} = 5.199$ Å, $a_{as} = 3.168$ Å) and the data suggest a reduction in the in-plane compressive stress. We have also probed the crystalline quality and stress in the porous film using micro-Raman scattering.

Figure 4 shows the Raman spectra of Si-doped porous GaN and as grown epilayer in the $z(xx)\bar{z}$ geometry. The spectra are dominated by strong E_2 and $A_1(LO)$ phonons near 568 and 734 cm^{-1}, which are in agreement with Raman selection rules for wurtzite GaN. As compared to the Raman spectrum of the as-grown film, a large increase in the scattering efficiency is clearly observed from the porous sample. An increase in the scattering signal has been observed previously for GaN nanocolumns.[24] Due to multiple scattering of light and more efficient coupling of the scattered radiation due to presence of surface disorder introduced by the surface nanostructuring, a significant enhancement of the Raman intensity is observed from porous film. The intensity is slightly lower in the case of undoped porous GaN film. However, the spectral lineshape is quite similar in both the porous samples. In GaN, the E_2 phonon

linewidth can be used to monitor the crystalline quality, while its frequency can be used to monitor the stress in the film. The E_2 phonon lines of GaN are observed at 569.2 and 568.1 cm^{-1} for the as grown and the Si-doped porous GaN sample, respectively. The red shift of 1.1 ± 0.2 cm^{-1} in the peak phonon frequency confirms the stress relaxation in porous GaN. This shift corresponds to a relaxation of compressive stress by 0.25 ± 0.05 GPa using the proportionality factor of 4.2 cm^{-1} GPa^{-1} for hexagonal GaN.[25] The starting as-grown n-GaN shows a compressive stress of about 0.41 GPa as estimated from Raman measurement. These observations show that stress relaxation estimated from PL and Raman shift agrees quite well. The fwhm value of E_2 phonon for as-grown and porous sample was 3.2 and 3.0 cm^{-1}, respectively, which shows that there is no difference in the phonon linewidth considering the spectral resolution of our Raman set up. Furthermore, such a lower value of the fwhm represents good crystalline quality. Anodization of the sample results in slight break down of the polarization selection rules, due to which very weak $E_1(TO)$ and $A_1(TO)$ modes also appeared in the spectrum recorded from porous film.

This comparative study using PL, XRD, and micro-Raman confirms that porous GaN layer possesses less compressive stress than as-grown GaN layer and the material uality of the porous sample is as good as the as-grown sample. PL intensity in porous GaN shows intensity enhancement at room temperature and a higher intensity enhancement at low temperature. Because band-edge PL is more surface-sensitive, presence of point defects or disorder in the top porous surface could lower the actual PL efficiency. From this study, we conclude that such strain released nanoporous GaN films prepared by photoelectrochemical etching can be used as an intermediate layer for overgrowth of GaN/InGaN/AlGaN layers for high luminescent device applications.

The Institute of Materials Research and Engineering assisted in meeting the publication costs of this article.

References

1. L. T. Canham, *Appl. Phys. Lett.*, **57**, 1046 (1990).
2. Y. H. Xie, W. L. Wilson, F. M. Ross, J. A. Mucha, E. A. Fitzgerald, J. M. Macaulay, and T. D. Harris, *J. Appl. Phys.*, **71**, 2403 (1992).
3. G. Oskam, A. Natarajan, P. C. Searson, and F. M. Ross, *Appl. Surf. Sci.*, **119**, 160 (1997).
4. P. Schmuki, D. J. Lockwood, H. J. Labbec, and J. W. Fraser, *Appl. Phys. Lett.*, **69**, 1620 (1996).
5. P. Schmuki, L. E. Erickson, D. J. Lockwood, J. W. Fraser, G. Champion, and H. J. Labbec, *Appl. Phys. Lett.*, **72**, 1039 (1998).
6. N. S. Averkiev, L. P. Kazakova, É. A. Lebedev, Yu. V. Rud', A. N. Smirnov, and N. N. Smirnova, *Semiconductors*, **34**, 732 (1999).
7. R. W. Tjerkstra, J. Go'mez Rivas, D. Vanmaekelbergh, and J. J. Kelly, *Electrochem. Solid-State Lett.*, **5**, G32 (2002).
8. A. F. Van Driel, B. P. J. Bret, D. Vanmaekelbergh, and J. J. Kelly, *Surf. Sci.*, **529**, 197 (2003).
9. A. F. van Driel, D. Vanmaekelbergh, and J. J. Kelly, *Appl. Phys. Lett.*, **84**, 3852 (2004).
10. S. Langa, I. M. Tiginyanu, J. Carstensen, M. Christophersen, and H. Föll, *Electrochem. Solid-State Lett.*, **3**, 514 (2000).
11. A. Liu and C. Duan, *Appl. Phys. Lett.*, **78**, 43 (2001).
12. G. Su, Q. Guo, and R. E. Palmer, *J. Appl. Phys.*, **94**, 7598 (2003).
13. C. K. Inoki, T. S. Kuan, C. D. Lee, A. Sagar, R. M. Feenstra, D. D. Koleske, D. J. Díaz, P. W. Bohn, and I. Adesida, *J. Electron. Mater.*, **32**, 855 (2003).
14. (a) M. Mynbaeva, A. Titkov, A. Kryzhanovski, I. Kotousova, A. S. Zubrilov, V. V. Ratnikov, V. Yu. Davydov, N. I. Kuznetsov, K. Mynbaev, D. V. Tsvetkov, S. Stepanov, A. Cherenkov, and V. A. Dmitriev, *MRS Internet J. Nitride Semicond. Res.*, **4**, 14 (1999); (b) M. Mynbaeva, A. Titkov, A. Kryganovskii, V. Ratnikov, K. Mynbaev, H. Huhtinen, R. Laiho, and V. Dmitriev, *Appl. Phys. Lett.*, **76**, 1113 (2000).
15. R. S. Qhalid Fareed, V. Adivarahan, C. Q. Chen, S. Rai, E. Kuokstis, J. W. Yang, M. Asif Khan, J. Caissie, and R. J. Molnar, *Appl. Phys. Lett.*, **84**, 696 (2004).
16. X. Li, Y. W. Kim, P. W. Bohn, and I. Adesida, *Appl. Phys. Lett.*, **80**, 980 (2002).
17. T. L. Williamson, D. J. Díaz, P. W. Bohn, and R. J. Molnar, *J. Vac. Sci. Technol. B*, **22**, 925 (2004).
18. D. J. Diaz, T. L. Williamson, I. Adesida, P. W. Bohn, and R. J. Molnar, *J. Vac. Sci. Technol. B*, **20**, 2375 (2002).
19. B. Yang and P. Fay, *J. Vac. Sci. Technol. B*, **22**, 1750 (2004).
20. I. M. Tiginyanu, V. V. Ursaki, V. V. Zalamai, S. Langa, S. Hubbard, D. Pavlidis, and H. Foll, *Appl. Phys. Lett.*, **83**, 1551 (2003).
21. Y. D. Wang, S. J. Chua, M. S. Sander, P. Chen, S. Tripathy, and C. G. Fonstad, *Appl. Phys. Lett.*, **85**, 816 (2004).
22. Y. P. Varshni, *Physica (Amsterdam)*, **34**, 149 (1967).
23. D. G. Zhao, S. J. Xu, M. H. Xie, S. Y. Tong, and H. Yang, *Appl. Phys. Lett.*, **83**, 677 (2003).
24. I. M. Tiginyanu, A. Sarua, G. Irmer, J. Monecke, S. M. Hubbard, D. Pavlidis, and V. Valiaev, *Phys. Rev. B*, **64**, 233317 (2001).
25. C. Kisielowski, J. Kruger, S. Ruvimov, T. Suski, J. W. Ager, E. Jones, Z. Liliental, M. Rubin, and E. R. Weber, *Phys. Rev. B*, **54**, 17745 (1996).